A Fast Algorithm for Determining the Propagation Path of Multiple Diffracted Rays

Patrizia Bagnerini, Annalisa Buffa, and Andrea Cangiani

***Abstract*—We present a fast algorithm for path computation of multiple diffracted rays relevant to ray tracing techniques. The focus is on double diffracted rays, but generalizations are also mentioned. The novelty of our approach is in the use of an analytical geometry procedure which permits to re-write the problem as a simple nonlinear equation. This procedure permits a convergence analysis of the algorithms involved in the numerical resolution of such nonlinear equation. Moreover, we also indicate how to choose the iteration starting point to obtain convergence of the (locally convergent) Newton method. As in previous works, explicit solutions are obtained in the relevant cases of parallel or incident diffraction edges.**

***Index Terms*—Electromagnetic edge diffraction, HF wave propagation, multiple diffraction, Newton method, ray tracing, urban propagation.**

I. Introduction

The numerical approximation of high frequency wave propagation is important in many applications as seismic, acoustic, optical waves and electromagnetics. The accuracy of direct numerical simulations depends on the number of grid points per wavelength, so that the computational cost increases with the frequency (see [1]). Thus, variants of geometrical optics are used. The main formulation of geometrical optics is *ray tracing* [1]–[3], where the solution is computed along the bi-characteristics of the Eikonal equation by solving a system of ordinary differential equations.

The aim of this work is to present a fast and robust method for the calculation of the path of multiple diffracted rays and to analyze the convergence of the proposed algorithms.

A relevant application is the accurate calculation of the electromagnetic field in wireless communications. In dense urban environments, multiple diffracted rays (for instance, at an edge of a building following a diffraction on the rooftop) are often the only or main contribution to an appreciable signal [4]. Moreover, the knowledge of the field is often required at many spatial points, hence it is essential for the single ray-tracing path to be calculated very efficiently.

Our algorithm can be used in *backward ray tracing* [2] techniques like *beam ray tracing* [5]–[7], i.e., whenever it is necessary to compute geometrical paths backwards from the receiver to the transmitter. The beam ray tracing method is based on the concept of illuminating beams, which are defined as portions of space that contain all the rays with the same interaction history. The evaluation of the illuminating beams involves the propagation through the environment of the information about the interactions between the propagating field and the environment. Once that all illuminating beams through the receiver have been found, the relevant paths are calculated going backwards from the receiver to the transmitter by determining the exact location of the reflections and diffractions on the given obstacles.

In backward ray tracing, multiple diffraction points can be analytically computed in the case of coplanar edges (incident or parallel), see [4], [8], and [9]. Analytical solution is not available for oblique edges: diffraction points are computed by solving a system of nonlinear equations with zero-searching methods, see e.g., [10]. A number of algorithms are proposed in the literature in order to minimize the computational cost. In [9], a one dimensional zero-searching algorithm is introduced in the case of second order diffraction. Higher order diffraction is treated by a recursive procedure which allows to exploit the closed form established for the second order case. In [6], the authors use a Newton scheme by taking the middle of the edges as initial points of the iteration. Since the equation satisfied by any diffraction point only depends on the previous and next diffraction points in the sequence, the Jacobian matrix is tridiagonal and can be evaluated analytically.

In this work, we propose an algorithm for the evaluation of double diffracted paths which permits to reduce the problem complexity of one dimension [9], by choosing an appropriate change of coordinates. An advantage of this approach is that it consents an analysis of the iterative algorithms and a proof of their convergence. We also indicate how to choose the iteration starting point to ensure convergence of locally convergent (but faster!) methods, like the Newton method. The algorithm applies to double diffracted rays, but generalizations are also discussed. As in [4], [8], [9], we furnish an analytical solution if the edges of diffraction are incident or parallel.

The paper is organized as follows. In Section II, we display the algorithm for multiple diffraction, whose construction is explained in Section III. The Section IV is devoted to the numerical schemes, with the analysis of their convergence. Numerical tests are also performed.

II. Problem Description and Solution Algorithm

We consider the problem of the evaluation of the path of a double diffracted ray travelling in empty space from a trans-

Manuscript received December 5, 2005; revised August 4, 2006. This work was supported by the Italian Ministry of Education, University and Research (MIUR) in the framework of the FIRB project RBNE01C79T.

P. Bagnerini is with Dipartimento di Ingegneria della Produzione, Termoenergetica e Modelli Matematici, Università di Genova, Genova 16129, Italy (e-mail: bagnerini@diptem.unige.it).

A. Buffa is with Istituto di Matematica Applicata e Tecnologie Informatiche del CNR, 27100 Pavia, Italy (e-mail: annalisa@imati.cnr.it).

A. Cangiani is with Dipartimento di Matematica, Università di Pavia, 27100 Pavia, Italy (e-mail: andrea.cangiani@unipv.it).

Digital Object Identifier 10.1109/TAP.2007.895543

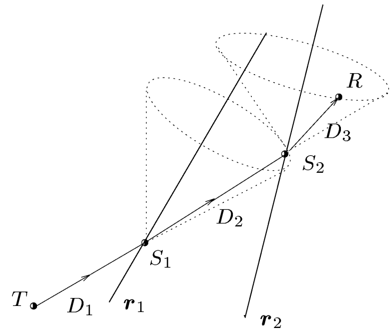

Fig. 1. Double diffraction path from the transmitter T to the receiver R.

mitter to a receiver whose positions are given. We deal with the case of infinite-length straight-edge diffraction.

Let $T = (t_1, t_2, t_3)$, $R = (r_1, r_2, r_3) \in \mathbb{R}^3$ be the location of the transmitter and the receiver, and let $\boldsymbol{r}_1$ and $\boldsymbol{r}_2$ be the two lines representing the edges of diffraction. Let S_1 and S_2 be the points of diffraction resp. in $\boldsymbol{r}_1$ and $\boldsymbol{r}_2$, as shown in Fig. 1. Physically, it is known that the ray follows a path of minimal length, hence S_1, S_2 may be found by minimization of

$$D(S_1, S_2) := \|S_1 - T\| + \|S_1 - S_2\| + \|S_2 - R\|$$

where $\|\cdot\|$ is the Euclidean norm. The existence and uniqueness of a minimizer follows from the strict convexity of D (see, e.g., [11]), as shown in the next proposition.

Proposition 1: Given T, $R \in \mathbb{R}^3$ *and two lines* $r_1 \neq r_2$ *such that* $T \notin r_1$ *and* $R \notin r_2$*, there is a unique piecewise rectilinear path from* T *to* R *through* r_1 *and* r_2 *of minimal length.*

Proof: Sum of convex functions is convex [11], and D_1, D_3 are clearly strictly convex. Hence it remains to show that D_2 is convex. To this end, given another couple of points $S_1' \in r_1$ and $S_2' \in r_2$ and their linear combination

$$S_1(\lambda) = \lambda S_1 + (1-\lambda) S_1'; \quad S_2(\lambda) = \lambda S_2 + (1-\lambda) S_2'$$

we have, $\forall \lambda \in [0, 1]$

$$\begin{aligned} S_2(\lambda) - S_1(\lambda) &= \lambda S_2 + (1-\lambda) S_2' - \lambda S_1 - (1-\lambda) S_1' \\ &= \lambda (S_2 - S_1) + (1-\lambda)(S_2' - S_1'). \end{aligned}$$

Then the triangle inequality implies the convexity of D_2. Strict convexity easily follows from the fact that D_1 and D_3, when considered as functions of $S_1 \in r_1$ and of $S_2 \in r_2$, respectively, are strictly convex. □

Remark: The proof naturally extends to the case of n *diffractions through infinite edges with* $n > 2$.

From the geometric theory of diffraction (GTD) [12], [13], we know that the diffraction points are also given as the points at which the angles formed between the edge and the incident and diffracted rays are equal. Applying this law one gets a system of two nonlinear equations for the positions of the diffraction points on the edges [8].

The novelty of our approach is that, before imposing that the angles are conserved, we perform an ad-hoc change of coordinates that permits to reduce the system of equations into a single

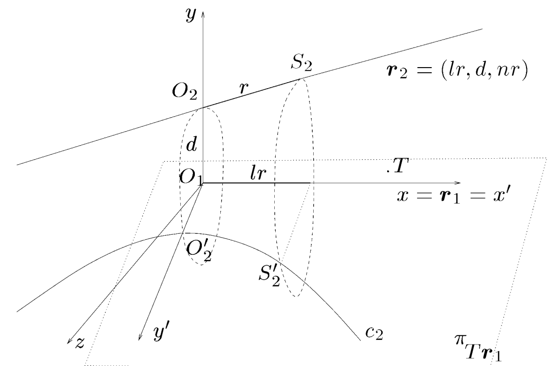

Fig. 2. The hyperbole c_2 is obtained by the rotation of the points of $\boldsymbol{r}_2$ around $\boldsymbol{r}_1$ until they belong to the plane containing T and $\boldsymbol{r}_1$.

equation. In this coordinate system, the starting point obtained by temporarily assuming coplanar edges is close enough to obtain the convergence of the Newton method.

Let $O_1 \in \boldsymbol{r}_1$ and $O_2 \in \boldsymbol{r}_2$ be the points of minimal distance between $\boldsymbol{r}_1$ and $\boldsymbol{r}_2$, and let $d = \mathrm{dist}(O_1, O_2)$. Consider a coordinate system with origin in the point O_1, first versor $\mathbf{e}_1$ along $\boldsymbol{r}_1$ and second versor $\mathbf{e}_2$ along the line segment of minimal distance, cf. Fig. 2. In a natural way, if $d = 0$, $\mathbf{e}_2$ is taken to be orthogonal to both lines.

With respect to such coordinate system, the line $\boldsymbol{r}_1$ corresponds to the x–axis and $\boldsymbol{r}_2$ is described by $d \in [0, +\infty)$ and the direction cosines $n \in (-1, 1]$ and $l = \sqrt{1 - n^2}$. The two lines admit the parametric representation $\boldsymbol{r}_1 : t \rightarrow (t, 0, 0)$ and $\boldsymbol{r}_2 : r \rightarrow (lr, d, nr)$. In turns, the points of diffraction are described as $S_1 = (t^*, 0, 0)$ and $S_2 = (lr^*, d, nr^*)$.

To determine the diffraction points we compute (r^*, t^*) by the following algorithm.

Algorithm $(S_1, S_2) = \texttt{doubled}(T, R, \boldsymbol{r}_1, \boldsymbol{r}_2)$

---

1. Compute the distance d, the direction cosines n, l and the locations

$$(T_1, T_2) = \left(t_1, -\sqrt{t_2^2 + t_3^2}\right)$$
$$(R_1, R_2) = (lr_1 + nr_3, -\|(r_1 - lR_1, r_2 - d, r_3 - nR_1)\|)$$

of the transmitter and receiver after an appropriate change of coordinates which superimpose in a single plane $\boldsymbol{r}_1$ with $\boldsymbol{r}_2$, see Section III.

2. If $d = 0$ (incident edges), then (r^*, t^*) is analytically obtained as the solution of the system of equations

$$\begin{cases} r = \frac{R_2 T_2 - (R_2 l - R_1 |n| \mathrm{sign}(t))(T_2 l - T_1 |n| \mathrm{sign}(r))}{R_2 |n| \mathrm{sign}(r) + |n| \mathrm{sign}(t)(T_2 l - T_1 |n| \mathrm{sign}(r))} \\ t = \frac{T_2 lr - T_1 |n||r|}{T_2 - |n||r|}. \end{cases} \tag{1}$$

3. If $d \neq 0$, then

a. If $n = 0$ (parallel edges), the solution is given by solving the linear system

$$\begin{cases} r = \frac{R_2 t - R_1 d}{R_2 - d} \\ t = \frac{T_2 r - T_1 d}{T_2 - d}. \end{cases} \tag{2}$$

b. If $n \neq 0$ (oblique edges), approximate (r^*, t^*) by using an iterative method to solve the system of nonlinear equations

$$\begin{cases} r = f_1(t) := \frac{R_2 lt - R_1 g(t)}{R_2 - g(t)} \\ t = f_2(r) := \frac{T_2 lr - T_1 g(r)}{T_2 - g(r)} \end{cases} \quad (3)$$

where $g(x) := \sqrt{d^2 + n^2 x^2}$. Equivalently, solve the fixed point equation

$$t = f(t) := f_2(f_1(t)). \quad (4)$$

Remark: In Section IV, we analyze some iterative algorithms for solving (4), proving their global convergence. Moreover, we recommend the use of the (locally convergent but faster) Newton method, as numerical evidence shows that choosing as starting point the solution obtained by temporarily putting $d = 0$ (step 2 in the algorithm above) guarantees convergence.

To compute the path of multiple diffracted rays, we can iterate the above algorithm (after all, this is obtained by superimposition of two single diffractions; see below). For instance, consider a triple diffracted ray and let S_1, S_2 and S_3 be the unknown diffraction points belonging to the edges $\boldsymbol{r}_1, \boldsymbol{r}_2$ and $\boldsymbol{r}_3$, respectively. We determine the diffraction points by the following iteration (`tol` is a given tolerance):

Algorithm $(S_1, S_2, S_3) = \texttt{tripled}\,(T, R, \boldsymbol{r}_1, \boldsymbol{r}_2, \boldsymbol{r}_3)$

1. Fix an initial guess for the position of S_3; initialize $S_2^{\rm old}$.

2. Compute

$$(S_1, S_2^1) = \texttt{doubled}\,(T, S_3, \boldsymbol{r}_1, \boldsymbol{r}_2)$$
$$(S_2^2, S_3) = \texttt{doubled}\,(S_1, R, \boldsymbol{r}_2, \boldsymbol{r}_3)$$

and set $S_2^{\rm new} = (S_2^1 + S_2^2)/2$.

3. If $\|S_2^{\rm new} - S_2^{\rm old}\|/\|S_2^{\rm new}\| \leq$ `tol` then $S_2 = S_2^{\rm new}$. Otherwise, $S_2^{\rm old} = S_2^{\rm new}$ and goto 2.

As before, if the edges are all parallel to each other, the solution is given by solving a linear system. Indeed, letting t, s and r be the positions of S_1, S_2 and S_3 on the respective edges, we have that

$$r = \frac{R_2 s - R_1 d_2}{R_2 - d_2}, \quad s = \frac{d_1 r + d_2 t}{d_1 + d_2}, \quad t = \frac{T_2 s - T_1 d_1}{T_2 - d_1}$$

where (T_1, T_2) and (R_1, R_2) represent the transmitter and the receiver in the coordinate systems which superimpose $\boldsymbol{r}_1$ with $\boldsymbol{r}_2$ and $\boldsymbol{r}_2$ with $\boldsymbol{r}_3$, respectively (cf. the construction below). Moreover, $d_1 = \text{dist}\,(\boldsymbol{r}_1, \boldsymbol{r}_2)$ and $d_2 = \text{dist}\,(\boldsymbol{r}_2, \boldsymbol{r}_3)$.

III. Algorithm Construction

Consider the problem of a single diffraction from the point T to the point R through an edge r. To obtain the diffraction point $S \in r$, we rotate, for instance, R around r, until it belongs to $\pi_{T,r}$, the plane containing T and r. Let R' be the rotated point. The location of the diffraction point is then obtained imposing the alignment of T, S, R'.

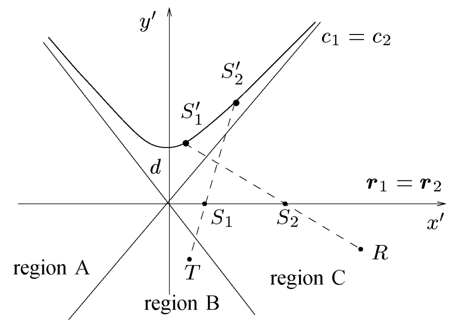

Fig. 3. The diffraction points S_1 and S_2 are obtained imposing the alignment of T, S_1, S_2' and R, S_2, S_1'. For future reference, the half-plane $y' < 0$ is subdivided into three regions determined by the asymptotes of the hyperbole.

We handle the double diffraction as two subsequent single diffractions. We rotate S_1 and S_2 around $\boldsymbol{r}_2$ and $\boldsymbol{r}_1$, respectively, and impose that T, S_1, S_2' and R, S_2, S_1' are aligned. This procedure leads to a system of two equations in the unknown positions of S_1 and S_2 on the edges.

If $n \neq 1$, rotating $\boldsymbol{r}_2$ around $\boldsymbol{r}_1$ we obtain an hyperboloid (a cylinder if the two lines are parallel). Instead, if $n = 1$, the two lines are orthogonal to each other, and rotating $\boldsymbol{r}_2$ around $\boldsymbol{r}_1$ we obtain a plane minus a discus of radii d.

Let us assume that $n \neq 1$, and consider the plane $\pi_{T,\boldsymbol{r}_1}$ containing T and $\boldsymbol{r}_1$. The intersection of such plane with the hyperboloid (resp. cylinder if $n = 0$) obtained rotating $\boldsymbol{r}_2$ around $\boldsymbol{r}_1$ is an hyperbole (resp. a line). In particular, we consider the branch of the hyperbole which is on the other side of T with respect to $\boldsymbol{r}_1$. This procedure is depicted in Fig. 2.

In the plane $\pi_{T,\boldsymbol{r}_1}$, we consider the coordinate system with origin in the point O_1, x$'$-axis along $\boldsymbol{r}_1$ and y$'$-axis such that the y$'$-coordinate of T is negative. In such coordinate system, the hyperbole is given by

$$c_2 : (y')^2 - \frac{n^2}{l^2}(x')^2 = d^2. \quad (5)$$

The correspondence between the points in $\boldsymbol{r}_2$ and their image in the hyperbole is given by

$$S_2 = (lr, d, nr) \in \boldsymbol{r}_2 \rightarrow S_2' = \left(lr, \sqrt{d^2 + (nr)^2}\right) \in \pi_{T,\boldsymbol{r}_1}. \quad (6)$$

Similarly, we can rotate $\boldsymbol{r}_1$ around $\boldsymbol{r}_2$ and consider c_1, the hyperbole obtained by intersection of the hyperboloid of rotation with the plane $\pi_{R,\boldsymbol{r}_2}$ containing R and $\boldsymbol{r}_2$. Further, with a change of coordinates, we can superimpose in a single plane $\boldsymbol{r}_1$ with $\boldsymbol{r}_2$ and c_1 with c_2, see Fig. 3. Notice that, after such change of coordinates, $O_1 \equiv O_2$. Moreover, T and R are in the half plane $y' \leq 0$; their exact location is specified in the algorithm above.

Remark: In the case $n = 1$, we can proceed in exactly the same way, only that, this time, the points S_1' and S_2' belong to the half-line $x' = 0$, $y' \geq d$.

The two points of diffraction S_1 and S_2 are now found by imposing that

$$T, S_1, S_2' \text{ are aligned and } R, S_2, S_1' \text{ are aligned.} \quad (7)$$

A possible configuration is depicted in Fig. 3.

In the plane, the correspondence of S_2' with S_2 [given by (6)] and of S_1' with S_1, reads

$$S_2 = (r, 0) \rightarrow S_2' = (lr, \sqrt{d^2 + n^2 r^2}) \tag{8}$$
$$S_1 = (t, 0) \rightarrow S_1' = (lt, \sqrt{d^2 + n^2 t^2}). \tag{9}$$

By imposing (7) and using (8) and (9), we obtain the system (3). In the analysis of (3), we distinguish the following cases.

- If $d = 0$ (incident edges), the system of (3) can be solved analytically. Notice that (0, 0) is always solution of (3). If (0, 0) is the only solution, then the minimum of D is attained there. Otherwise, the system of (3) has a solution different from (0, 0) which corresponds to the unique minimum of D.
- If $d \neq 0$, as discussed in the previous Section, the existence of a unique extremal for the function D ensures that (3) has a unique solution (fixed point). This case is treated in the next section.

IV. Numerical Algorithms: Description and Convergence

In what follows, we consider the case where no analytical solution is available, i.e., we assume that $d, n \neq 0$.

The action of the function f which, in general, is not a contraction, is described by the following steps (here, the points are identified with their x'–components), see Fig. 3.

1. Given $t \in \mathbb{R}$, set $S_1' = lt$;

2. $S_2 = \text{intersection of the line } r_{R,S_1'}$ with the x'–axis (where $r_{R,S_1'}$ is the straight line passing by R and S_1');

3. Similarly, from S_2, complete the process by setting $S_1 = \text{intersection of the line } r_{T,S_2'}$ with the x'–axis.

Let A, B, C the subregions of the semi-plane $y' < 0$ determined by the asymptotes of the hyperbole, cf. Fig. 3. Following the previous description, and depending on the displacement of T and R inside the three regions, we can fully characterize the functions f_1 and f_2.

For instance, consider the function f_1 and assume $R \in A$. Letting t varying from $-\infty$ to $+\infty$, the point S_1' moves from left to right along the hyperbole. The position of S_2 in the x–axis, i.e., $f_1(t)$, is monotonically decreasing until the value t where the line $r_{R,S_1'}$ is tangent to the hyperbole, and is monotonically increasing afterwords.

All possible behaviors of f_1, f_2 are represented in Fig. 4 and summarized in the following proposition.

Proposition 2: The following properties hold.

1. The functions $f, f_1, f_2 \in \mathcal{C}^1(\mathbb{R})$ and are bounded.
2. The functions f_1 and f_2 have at most one extrema. In particular, R (resp. T) $\in A \Rightarrow f_1$ (resp. f_2) < 0 has a maximum at some $x > 0$, R (resp. T) $\in B \Rightarrow f_1$ (resp. f_2) is strictly monotone increasing, R (resp. T) $\in C \Rightarrow f_1$ (resp. f_2)> 0 has a minimum at some $x < 0$.
3. Let t^* be the solution of (4), i.e., $t^* = f(t^*)$. Then $0 \leq f'(t^*) \leq 1$, where f' denotes the derivative of f.

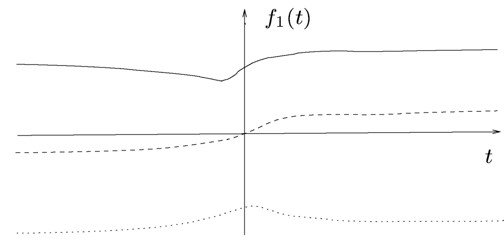

Fig. 4. The behavior of f_1 in function of the position of the receiver R resp. in the region A (dotted line), B (dashed line), and C (solid line), also cf. Fig. 3. The function f_2 has an identical dependency on T.

Moreover

$$t > t^* \Rightarrow t > f(t) \quad \text{and} \quad t < t^* \Rightarrow t < f(t). \tag{10}$$

Proof: The inequality $f'(t^*) \leq 1$ and (10) follow easily from the continuity and boundedness of f, the continuity of f' and the uniqueness of t^* as solution of (4). To prove that $f'(t^*) \geq 0$ we proceed as follows. We have $f'(t^*) = f_2'(r^*) f_1'(t^*)$, thus we just need to show that $f_1'(t^*)$ and $f_2'(r^*)$ have the same sign. For any given $t \in \mathbb{R}$ we have

$$f_1'(t) = -R_2 \frac{-R_2 l g(t) + d^2 l + R_1(1 - l^2)t}{g(t)(R_2 - g(t))^2}.$$

Further, we obtain R_1 from the definition of $f_1(t)$

$$R_1 = \frac{-(R_2 - g(t)) f_1(t) + R_2 lt}{g(t)}$$

and, after substitution, we get

$$f_1'(t) = \frac{R_2}{g(t)^2 (R_2 - g(t))} \left(d^2 l + (1 - l^2) f_1(t) t \right). \tag{11}$$

Similarly, for any $r \in \mathbb{R}$

$$f_2'(r) = \frac{T_2}{g(r)^2 (T_2 - g(r))} \left(d^2 l + (1 - l^2) r f_2(r) \right). \tag{12}$$

Since $g > 0$ and $R_2, T_2 < 0$, the sign of $f_1'(t)$ and $f_2'(r)$ is equal to the sign of the second term in (11) and (12), respectively. We now concentrate our attention on the fixed point (r^*, t^*). Since $f_1(t^*) = r^*$ and $f_2(r^*) = t^*$, from (11) and (12) it follows that the two derivatives have the same sign at the fixed point. □

In order to solve (4), we list a couple of methods for which, using in different ways the properties of the function f listed above, we can prove global convergence.

1) Regula Falsi: Let $F(t) = t - f(t)$. Given an interval $I = (t^0, t^1)$ such that $t^* \in I$ and $F(t^0)F(t^1) < 0$, the regula falsi method is

$$t^{k+1} = t^k - \frac{t^k - t^{k'}}{F(t^k) - F(t^{k'})} F(t^k) \qquad k \geq 1$$

with k' being the maximum index less than k such that $F(t^{k'})F(t^k) < 0$. For the (4), we can take $I := f_2(f_1(\mathbb{R})) \subset \mathbb{R}$,

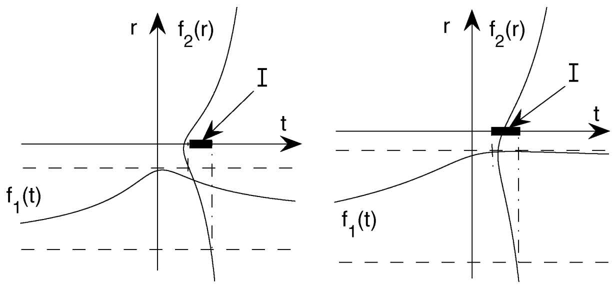

Fig. 5. Depiction of the interval $I = f_2(f_1(\mathbb{R}))$ when the function f_1 has a maximum and f_2 a minimum. In the case represented on the left plot (corresponding to $f_1'(t^*), f_2'(r^*) < 0$), their composition $f = f_2 \circ f_1$ is monotone in I, while in the case represented on the right plot (corresponding to $f_1'(t^*), f_2'(r^*) > 0$), f has a maximum in I, due to the maximum of f_1 being attained inside I.

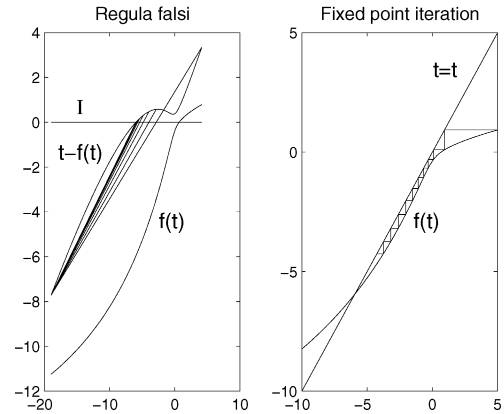

Fig. 6. Few iterates of both the regula falsi (left) and fixed point (right) algorithms given the same data configuration.

since I can be obtained by calculating maxima, minima and limits of f_1 and f_2, cf. the examples in Fig. 5.

This algorithm is an always convergent variant of the secant method. If f does not change convexity in I, convergence is linear, cf. [14]. In the vicinity of the solution one should switch to faster algorithms like for instance, the secant or Newton method. Any bisection-kind algorithm may be used as an alternative to regula falsi.

2) Fixed Point Iteration: Given $t^0 \in \mathbb{R}$, for $k = 0, 1, 2, \ldots,$ we let

$$t^{k+1} = f(t^k). \tag{13}$$

Proposition 3 ensures that t^* is a point of attraction of the fixed point iteration, i.e., (13) is locally convergent. The following proposition shows that convergence is global.

Proposition 3: For any $t^0 \in \mathbb{R}$ the fixed point iteration (13) converges to the unique fixed point t^* of (4).

Proof: Let $I = f_2(f_1(\mathbb{R}))$ be the interval considered above. Since the first iteration of (13) will always fall into I, and the iterates generated by (13) cannot leave such interval, we only need to prove convergence in I. By examining the behavior of $f|_I = f_2 \circ f_1 : I \to \mathbb{R}$ case-by-case with respect to the classification given in Proposition 2, one can see that, at least on one side of t^*, the function $f|_I$ is monotone (see Fig. 5 for a couple of examples).

Assume, for instance, that $f(t)$ is monotone on $I^+ = \{t \in I : t \geq t^*\}$. In particular, f must be monotonic increasing in I^+. If $t^0 \in I^+$, from (10) and the monotonicity of f, it follows that the fixed point iteration monotonically converges in I^+, see e.g., [15, p. 283]. If, instead, $t^0 \notin I^+$, two cases may occur:

i) there exist a $k \in \mathbb{N}$ such that $t^k > t^*$, and thus monotonic convergence follows from this iterate onwards since $t^k \in I^+$;
ii) $t^k \leq t^*$ for all $k \in \mathbb{N}$. In this case, due to (10), $t^k \leq t^{k+1} = f(t^k) \leq t^*$, with equality only if $t^k = t^*$. Thus, t^k represents a monotone sequence bounded by t^*. Since t^* is the unique accumulation point of f, it follows that $t^k \to t^*$.

□

The fixed point iteration can exhibit arbitrarily slow convergence, the asymptotic rate of convergence being equal to $-\log 1/|f'(t^*)|$, see [16] and [14]. This fact is nicely depicted in Fig. 6. Acceleration can be achieved by over-relaxation.

3) Newton Method: The solution of (4) presents some difficulties only when $d \ll 1$, due to the presence, when $d = 0$, of two solutions (fixed points), one of which is $t = 0$. This difficulty is nicely depicted in Fig. 6. We propose to solve the (4) by the Newton method, using as starting point t_0 the value obtained by temporarily assuming $d = 0$ (see step 2 of the algorithm): we take as t_0 the unique non-zero solution of (1), if it exists and the mid point of the edge, otherwise. Roughly speaking, if the distance $d \ll 1$, then the starting point obtained by imposing $d = 0$ is close enough to the solution to ensure convergence. Otherwise, the nice behavior of f ensures global convergence, hence the choice of the starting point is irrelevant.

To confirm this ansatz, we apply the Newton method and the fixed point method to the solution of (4) as d varies. The other parameters are kept constant and correspond to the data configuration of Case 1 in Table II, see also Fig. 7. In Table I, we report the distance d between the two edges, the starting point t^0, the fixed point t^*, the difference between them in absolute value and the number of iterations necessary to reach machine-precision set to 10^{-14}. The experiment shows that, with our choice for the iteration initial guess, the Newton method converges robustly in d. This is not verified if we take a randomly chosen point or, for instance, the mid point of the edge.

We also tested the algorithm on some extreme configurations corresponding to the data-sets reported in Table II, see also Fig. 7. In particular, we fixed the transmitter and receiver positions distant less then 10^{-8} from the hyperbole asymptotes (Case 2), near to the x-axis (Case 3) and, finally, far from the origin (Case 4). Starting from our carefully chosen initial guess t^0, the Newton method always converges quadratically.

To further ascertain the algorithm robustness, we test it on a large number of randomly generated configurations. The problem configurations are obtained by generating randomly the coordinates of the transmitter, the receiver and two points per edge defining them. The coordinates are randomly uniformly distributed in the 10^3 box centered in the origin. The algorithm performances actually proved independent of the distance between the transmitter and receiver and the edges configuration. The algorithm needs 4 Newton iterations in average to reach machine-precision, see Table III.

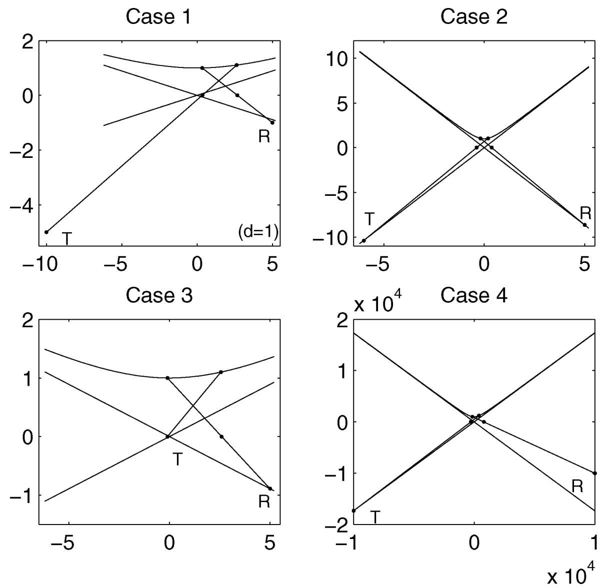

Fig. 7. Test configurations and solution for the test-cases in Table II.

TABLE I
NEWTON AND FIXED POINT ITERATIONS NEEDED TO REACH MACHINE PRECISION STARTING FROM THE PROPOSED INITIAL GUESS t^0. CASE 1: $T = (-10, -5), R = (5, -1), l = 0.98455$

d	t^0	t^*	$\|t^0 - t^*\|$	iter-NEW	iter-FP
.001	0.74893	0.74895	1.72e-05	2	52
.01	0.74893	0.75063	1.7e-03	3	53
.1	0.74893	0.84201	9.3e-02	4	52
1	0.74893	0.34678	4.02e-1	3	29
10	0.74893	-5.33841	6.08	3	10
100	0.74893	-9.29598	10.04	2	5
1000	0.74893	-9.92582	10.67	2	3

TABLE II
NEWTON ITERATIONS NEEDED TO REACH MACHINE PRECISION FOR SOME TEST-CASES CONFIGURATIONS

Config.	T	R	l	d	iter-NEW
Case 1	$-(10, 5)$	$(-5, -1)$	0.98	vary	Table I
Case 2	$-(6, 10.4$	$(5, -8.66)$	.5	1	5
Case 3	$-(0.1, 10^{-4})$	$(5, -0.889)$	0.98	1	2
Case 4	$10^4(1, -1.7)$	$10^4(1, -1)$	0.5	10^3	5

TABLE III
AVERAGE NUMBER OF NEWTON ITERATIONS OVER A LARGE NUMBER OF RANDOMLY GENERATED CONFIGURATIONS

tol	runs	max-iter-NEW	iter-NEW
10^{-14}	10000	9	3.984

TABLE IV
TRIPLE DIFFRACTION: AVERAGE NUMBER OF NEWTON ITERATIONS

tol	runs	max-iter-NEW	ext-iter-NEW	int-iter-NEW
10^{-4}	10^4	15	3.9	33
10^{-6}	10^4	18	5	41.8
10^{-8}	10^4	24	6	50.4
10^{-10}	10^4	39	7	58.6
10^{-12}	10^4	37	8	67.1

Finally, we test the triple diffraction algorithm of Section II. As before, we generate a large number of test configurations using randomly generated coordinates. The convergence results are reported in Table IV where "ext-iter-NEW" denotes the average number of exterior loops for the algorithm tripled, whereas in "int-iter-NEW" we average the total number of interior loops (iterations inside any call to doubled). In all loops we use our Newton strategy. The test indicates linear error reduction, although in few cases the number of iterations is quite larger than average, as shown by the maximum number of iterations "max-iter-NEW" also reported in the Table. It was not possible to reduce the error to machine precision, due to the errors coming from the alternated solution of the nested double diffractions (see [17] for a discussion about this phenomenon). The Matlab code of double and triple diffraction are available on the following webpage: http://www.imati.cnr.it/analisa/CODES/diffraction.html

V. CONCLUSION

We have presented some algorithms to speed-up numerical computation of multiple diffracted rays in backward ray tracing techniques.

The algorithms are based on reducing the relevant problem complexity of one dimension by performing a suitable change of coordinates. A further advantage of this approach is that it permits the numerical analysis of the algorithms. We proved global convergence to the analytical solution. Moreover, in the new coordinate system, the value obtained by temporarily assuming coplanar edges provides a good starting point for the (locally convergent) Newton algorithm.

ACKNOWLEDGMENT

The authors thank Dr. L. Valbonesi for presenting them with the problem studied in this paper and Prof. F. Brezzi for useful discussions and suggestions.

REFERENCES

[1] B. Engquist and O. Runborg, "Computational high frequency wave propagation," *Acta Numerica*, pp. 1–86, 2003.

[2] A. S. Glassner, *An Introduction to Ray-Tracing*. San Diego, CA: Academic, 1989.

[3] R. T. Langan, I. Lerche, and R. T. Cutler, "Tracing of rays through heterogeneous media: An accurate and efficient procedure," *Geophysics*, vol. 50, pp. 1456–1465, 1985.

[4] S. Y. Tan, T. W. Ang, and H. S. Tan, "Measurement validation of ray-tracing propagation model on double-diffracted paths," *IEEE Trans. Antennas Propag.*, vol. 50, pp. 411–413, 2002.

[5] L. Valbonesi, "A new approach for electromagnetic field evaluation in urban environments: Beam ray tracing," presented at the IEEE Int. Conf. on Electromagnetics in Advanced Applications (ICEAA), Torino, Italy, Sep. 10-14, 2001.

[6] T. Funkhouser, N. Tsingos, I. Carlbom, G. Elko, M. Sondhi, J. E. West, G. Pingali, P. Min, and A. Ngan, "A beam tracing method for interactive architectural acoustics," *J. Acoust. Soc. Amer.*, vol. 115, no. 2, pp. 739–756, 2004.

[7] G. Liang and H. L. Bertoni, "A new approach to 3-D ray tracing for propagation prediction in cities," *IEEE Trans. Antennas Propag.*, vol. 46, no. 6, pp. 853–863, 1998.

[8] T. W. Ang, S. Y. Tan, and H. S. Tan, "Analytical methods to determine diffraction points on multiple edges and cylindrical scatterers in UTD ray tracing," *Microw. Opt. Technol. Lett.*, vol. 22, no. 5, pp. 304–309, 1999.

[9] E. Di Giampaolo and F. Bardati, "Analytical model of multiple wedge-diffracted ray congruence," *Electromagn.*, vol. 23, no. 6, pp. 509–523, 2003.

[10] M. F. Catedra and J. Pérez-Arriaga, *Cell Planning for Wireless Communications*. Boston, MA: Artech House, 1999, vol. 28.

[11] I. Ekeland and R. Témam, *Convex Analysis and Variational Problems*. Philadelphia, PA: SIAM, 1999, vol. 28, Classics in Applied Mathematics.

[12] J. B. Keller, “Geometrical theory of diffraction,” *J. Opt. Soc. Amer.*, vol. 52, pp. 116–130, 1962.
[13] R. G. Kouyoumjian and P. H. Pathak, “A uniform geometrical theory of diffraction for an edge in a perfectly conducting surface,” *Proc. IEEE*, vol. 62, pp. 1448–1461, 1974.
[14] J. Stoer and R. Bulirsch, *Introduction to Numerical Analysis*. New York: Springer-Verlag, 2002, vol. 12, Texts in Applied Mathematics.
[15] E. Zeidler, *Nonlinear Functional Analysis and its Applications. I*. New York: Springer-Verlag, 1986.
[16] A. Quarteroni, R. Sacco, and F. Saleri, *Numerical Mathematics*. New York: Springer-Verlag, 2000, vol. 37, Texts in Applied Mathematics.
[17] E. D. Giampaolo, M. Sabbadini, and F. Bardati, “Astigmatic beam tracing for GTD/UTD methods in 3-D complex environments,” *J. Electromagn. Waves Applicat.*, vol. 15, pp. 439–460, 2001.

Annalisa Buffa received the Ph.D. degree in mathematics from the University of Milan, Italy, in 2000 and the Dr.Sc. degree in computer science engineering from the University of Pavia, Italy, in 1996.

From 2001 to 2004, she was a Researcher in applied mathematics at the Institute of Numerical Analysis of the Italian National Research Council (CNR), Pavia, Italy. Since 2004, she has been a Research Director (equivalent to full Professor) at the Institute of Applied Mathematics and Information Technology of CNR. Since 2001, she was an invited professor at several universities including ETH-Zurich, Switzerland; École Polytéchnique and the University of Paris VI, France; and ICES-University of Texas at Austin. Currently, her main scientific interests are in the field of computational electromagnetism with variational technique, i.e., finite and boundary elements. She works actively on the definition and the mathematical wellposedness of integral equations for electromagnetic wave propagation in exterior domains, in presence of dielectric interfaces and antennas, and eigenvalues problems for waveguides. In the past, she worked intensively on discretization methods for eddy-currents problems with moving geometries, and on mathematical justifications of low frequency models in electromagnetics. She has coauthored more than 40 papers in journals and international publications on different subjects including applied mathematics, numerical analysis, and computational electromagnetism.

Patrizia Bagnerini received the Ph.D. degree in numerical analysis from the University of Nice, France, in 2002 and the Dr.Sc. degree in applied mathematics from the University of Genova, Italy, in 1994. Her Ph.D. thesis concerned adaptive mesh generation by using Hamilton–Jacobi equations and hyperbolic traffic flow problems.

From 2003 to 2005, she held a Postdoctoral position in the applied mathematics at the University of Pavia, Italy. Since 2005, she has been a Researcher in the Faculty of Engineering of Genova. She is the author of research papers in mesh generation and hyperbolic problems. Currently, her scientific interests concern traffic flow models and adaptive mesh generation applied to prefractal transmission problems. She is also working on a joint project with the Department of Mathematics and the Institute of Signalling, Developmental Biology and Cancer of Nice, on a mathematical model of dorsal closure of drosophila (a paradigm to study the sealing of epithelial sheets).

Andrea Cangiani was born in Milan, Italy, in 1972. He received the Laurea degree in mathematics from the University of Trento, Italy, in 1999 with a thesis on DDM methods in electromagnetics, and the M.Sc. degree in mathematical modelling and scientific computing with a dissertation on mathematical finance and the D.Phil. degree in numerical analysis with a thesis on stabilized FEMs for multiscale problems both from Oxford University, Oxford, U.K., in 2000 and 2004, respectively.

He is currently with the Mathematics Department of Pavia University, Italy, which he joined as a Postdoctoral Researcher in 2004. His scientific interests are in the field of numerical analysis for fluid dynamics and electromagnetism. He is the author of research papers in mesh adaptivity and numerical analysis of stabilized finite element methods, and he is currently researching mimetic finite difference methods.

Dr. Cangiani received the Oxford University Nuclear Electric Prize in 2000.